Wavelet and neuro-fuzzy conjunction model for streamflow forecasting

Özgür Kişi and Turgay Partal

ABSTRACT

In this study the wavelet-neuro-fuzzy model, which combines the wavelet transform and the neuro-fuzzy technique, has been employed to forecast monthly streamflows. The observed monthly streamflow data are decomposed into some sub-series (components) by discrete wavelet transform and then appropriate sub-series are used as inputs to the neuro-fuzzy models for forecasting monthly streamflows. The data from two stations, Durucasu and Tanir, in Turkey are used as case studies. The wavelet-neuro-fuzzy forecasts are compared with those of the single neuro-fuzzy models. Comparison results indicate that the wavelet-neuro-fuzzy model is superior to the classical neuro-fuzzy method especially for the peak values. For the Durucasu and Tanir stations, it was found that the wavelet-neuro-fuzzy models are superior in forecasting monthly streamflows than the optimal neuro-fuzzy models.

Key words | discrete wavelet transform, forecast, neuro-fuzzy, streamflow

Özgür Kişi (corresponding author)
Civil Engineering Department,
Engineering Faculty, Hydraulics Division,
Erciyes University,
38039, Kayseri,
Turkey
E-mail: *kisi@erciyes.edu.tr*

Turgay Partal
Civil Engineering Department,
Engineering Faculty,
Dumlupinar University,
Kutahya,
Turkey

INTRODUCTION

Hydrologists believe that flow processes are highly non-linear, spatially distributed and time varying. Forecasting magnitude of streamflows for short term and long term such as months or possibly longer is required for planning or designing of water resources systems (Zealand *et al.* 1999). Monthly streamflow prediction has a significant importance in water resource system planning, because storage-yield sequences are generally related to monthly periods (Cannas *et al.* 2006).

Artificial neural networks (ANNs) have been successfully studied forecast/estimate various hydrological variables. ANN models have been employed for rainfall–runoff forecasting (Hsu *et al.* 1995; Tokar & Johnson 1999; Antar *et al.* 2006), for river flow prediction (Zealand *et al.* 1999; Sivakumar *et al.* 2002; Kumar *et al.* 2004; Kisi 2004a, 2008; Cigizoglu 2005; Cigizoglu & Kisi 2005; Sivakumar 2005; Iliadis & Maris 2007; May & Sivakumar 2009), for precipitation forecasting (Hall 1999; Ramirez *et al.* 2005; Freiwan & Cigizoglu 2005), and for sediment prediction (Kisi 2004b; Cigizoglu & Kisi 2006; Alp & Cigizoglu 2007).

Neuro-fuzzy models have been successfully used in the hydrological sciences during recent years. Nayak *et al.* (2004) evaluated the potential of neuro-fuzzy technique in forecasting river flow time series. Kisi (2005) used a neuro-fuzzy model for daily suspended sediment estimation. Nayak *et al.* (2005) used a neuro-fuzzy model for short-term flood forecasting. Kisi (2006) investigated the accuracy of neuro-fuzzy computing technique in daily evaporation modeling. Chang & Chang (2006) used a neuro-fuzzy approach to construct a water level forecasting system during flood period. Kisi & Ozturk (2007) investigated the accuracy of adaptive neuro-fuzzy method for modeling reference evapotranspiration.

In the last decade, wavelet transforms have become a useful method for analyzing such as variations, periodicities, trends in time series (Torrence & Compo 1998; Smith *et al.* 1998; Lu 2002; Xingang *et al.* 2003; Coulibaly & Burn 2004; Yueqing *et al.* 2004; Partal & Küçük 2006). In recent years, some hybrid models of wavelet transform have been improved for prediction (Li *et al.* 1999; Zheng *et al.* 2000; Zhang & Dong 2001). Especially, wavelet-ANN models have been employed in some studies in hydrology and water resources successfully (Kim & Valdes 2003;

doi: 10.2166/nh.2011.048

Wang & Ding 2003; Anctil & Tape 2004). It is seen from these studies that the wavelet transform fairly improves forecasting accuracy. Partal & Kisi (2007) first proposed a new conjunction method (the wavelet-neuro-fuzzy model) for daily precipitation forecasting.

Wavelet transforms provides useful information about the structure of the physical process to be modeled. Discrete wavelet transform is considered for decomposition of signal. Sub-series decomposed by discrete wavelet transform from original time series provide detailed information about the data structure and its periodicity (Wang & Ding 2003). The attribute of each sub-series is distinct. Wavelet components of original time series improve the ability of a forecasting model by giving useful information on various resolution levels (Kim & Valdes 2003). Therefore, coupling wavelets with neuro-fuzzy may provide significant advantages.

In the present study, the conjunction model (wavelet-neuro-fuzzy) is applied for forecasting monthly streamflows of Turkey. For this aim, streamflow data are first decomposed into wavelet sub-series by discrete wavelet transform. Then, the neuro-fuzzy model is constructed by using appropriate wavelet sub-series inputs, and observed streamflow time series output. Finally, the accuracy of the wavelet-neuro-fuzzy conjunction model is compared with that of the single neuro-fuzzy model. This study is the first application for flow forecasting using wavelet and neuro-fuzzy in the literature.

DATA AND STATISTICAL ANALYSIS

The monthly streamflow data of two stations, Durucasu Station (Station No: 1413) on Yesilirmak River at Yesilirmak Basin in the North Anatolia Region of Turkey and

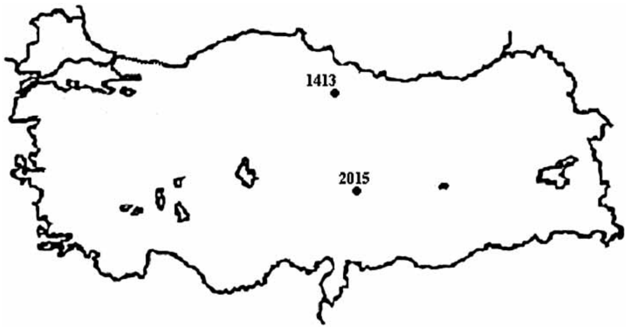

Figure 1 | Location map of the streamflow stations.

Tanir Station (Station No: 2015) on Hurman River at Ceyhan Basin in the Center Anatolia Region of Turkey, are used in the study (Figure 1). The precipitation area of the station 1413 is approximately 21,600 km^2 and its elevation is 25 m, while the precipitation area of the station 2015 is approximately 900 km^2 and its elevation is 1,100 m. The monthly data records which cover a time period of 35 years (420 months) from January 1962 to December 1996 are obtained from DSI (General Directorate of State Hydraulics Works).

Related information for the streamflow data is presented in Table 1. Some statistical parameters (mean, maximum, standard deviation, skewness, lag-1, lag-2 and lag-3 autocorrelation coefficients) for the training, testing and whole data are shown in the table. Station 1413 has the highest monthly streamflow value ($x_{max} = 350.20$ m^3/s for whole data of station 1413). It can be seen from the skewness coefficients in the sixth column of Table 1 that the streamflow data show scattered distribution. The lag-2 and lag-3 auto-correlations are quite low showing low persistence (e.g. $r_2 = 0.35$, $r_3 = 0.04$). The lag-1 auto-correlation of

Table 1 | Related information for the river flow stations. Besides, some statistical parameters of the monthly flow data (x_{mean}, x_{max}, s_x, c_{sx}, r_1, r_2, r_3 denote mean, maximum, standard deviation, skewness, lag 1, lag 2 and lag 3 autocorrelation coefficients, respectively)

Station	Data set	x_{mean} (m^3/s)	x_{max} (m^3/s)	s_x (m^3/s)	c_{sx}	r_1	r_2	r_3
1413	Training data	71.50	350.20	56.46	1.59	0.72	0.36	0.05
	Testing data	60.98	286.00	58.57	2.07	0.65	0.27	−0.01
	Whole data	69.40	350.20	56.97	1.67	0.71	0.35	0.04
2015	Training data	8.94	39.30	5.91	2.16	0.72	0.37	0.11
	Testing data	7.56	25.10	4.71	1.94	0.72	0.27	−0.03
	Whole data	8.66	39.30	5.71	2.16	0.73	0.36	0.10

the monthly streamflow records has a significant value (e.g. $r_1 = 0.71$).

METHODS

Wavelet analysis

The wavelet transform is a strong mathematical tool that provides a time–frequency representation of an analyzed signal in the time domain (Daubechies 1990). In recent years, there has been an increasing interest in the use of wavelet analysis in a wide range of fields for water resources and meteorology (Smith *et al.* 1998; Park & Mann 2000; Kucuk 2004; Yan *et al.* 2004). Wavelet transform analysis, developed during the last two decades, appears to be a more effective tool than the Fourier transform (FT) in studying non-stationary time series. The results in a plot of energy versus frequency for the energy spectrum in FT and fast FT (FFT), the wavelet spectrum is three-dimensional and, thus, energy appears as contour lines plotted in the time–frequency domain. Of course, this provides an ideal opportunity to examine the process of energy variations in terms of where and when hydrological events occur (Küçük & Ağıralioğ 2003; Partal & Kisi 2007).

Discrete wavelet transform

Calculating the wavelet coefficients at every possible scale is a fair amount of work, and it generates a lot of data. If one chooses scales and positions based on the powers of two (*dyadic* scales and positions) then the analysis will be much more efficient as well as accurate. This transform is called the discrete wavelet transform, and has the form

$$\psi_{m,n}\left(\frac{t-\tau}{s}\right) = s_0^{-m/2}\psi\left(\frac{t-n\tau_0 s_0^m}{s_0^m}\right) \quad (1)$$

where m and n are integers that control respectively the wavelet dilation (scale) and translation (time); s_0 is a specified fixed dilation step greater than 1; and τ_0 is the location parameter and must be greater than zero. From this equation, it can be seen that the translation step, $n\tau_0 s_0^m$, depends on the dilation, s_0^m. The most common (and simplest) choice for the parameters s_0 and τ_0 is 2 and 1 (time steps), respectively. This power of two logarithmic scaling of the translations and dilations is known as dyadic grid arrangement and is the simplest and most efficient case for practical purposes (Mallat 1998). For a discrete time series x_i, where x_i occurs at discrete time i (i.e. here integer time steps are used), the discrete wavelet transform becomes

$$W_{m,n} = 2^{-m/2}\sum_{i=0}^{N-1} x_i \psi(2^{-m}i - n) \quad (2)$$

where $W_{m,n}$ is wavelet coefficient for the discrete wavelet of scale $s = 2^m$ and location $\tau = 2^m n$.

Thus, the discrete wavelet transform provides information about the variation in a time series at different scales and locations as defined above (Partal & Kisi 2007).

Adaptive neuro-fuzzy inference system

The adaptive neuro-fuzzy inference system (ANFIS), first introduced by Jang (1993), is a universal approximator and as such is capable of approximating any real continuous function on a compact set to any degree of accuracy (Jang *et al.* 1997). ANFIS is functionally equivalent to fuzzy inference systems (Jang *et al.* 1997). Specifically the ANFIS system of interest here is functionally equivalent to the Sugeno first-order fuzzy model (Jang *et al.* 1997; Drake 2000). Below, the hybrid learning algorithm, which combines gradient descent and the least-squares method, is introduced.

As a simple example we assume a fuzzy inference system with two inputs x and y and one output f. The first-order Sugeno fuzzy model, a typical rule set with two fuzzy If-Then rules can be expressed as:

Rule 1: If x is A_1 and y is B_1, then

$$f_1 = p_1 x + q_1 y + r_1 \quad (3)$$

Rule 2: If x is A_2 and y is B_2, then

$$f_2 = p_2 x + q_2 y + r_2 \quad (4)$$

where A_1, A_2 and B_1, B_2 are the membership functions for inputs x and y, respectively, and p_1, q_1, r_1 and p_2, q_2, r_2 are the parameters of the output function. The output f is the weighted average of the individual rule outputs and is itself a crisp value. The functioning of the ANFIS can be found in Jang (1993) and Partal & Kisi (2007).

HOW IS THE WAVELET-NEURO-FUZZY MODEL EMPLOYED?

The wavelet-neuro-fuzzy conjunction model combines two methods, discrete wavelet transform and neuro-fuzzy techniques. Here, observed flow data is decomposed into sub-series by the wavelet technique. The decomposed wavelet components (D) are new time series and have different contribution on the observed series. Then, the appropriate D components are selected as inputs of neuro-fuzzy model for forecasting monthly streamflows. For the selection of appropriate (dominant) the D components, the correlation coefficients between Ds and observed streamflow data are calculated. So that, the new series obtained by adding the dominant Ds is used as the conjunction model input. As results, the wavelet and neuro-fuzzy model goals to forecast one-month-ahead flows employing sub-series components (Ds) obtained using discrete wavelet transform on original data.

APPLICATIONS

Wavelet decomposition of observed time series

The monthly streamflow data is decomposed into different sub-time series (Ds) at distinct resolution level by the discrete wavelet transform. The signal is decomposed into series of approximation and details by following Mallat's algorithm. The process consists of a number of successive filtering steps. The signal is first decomposed into an approximation and accompanying detail. The decomposition process is then iterated, with successive approximation being decomposed in turn, so that the original signal is broken down into many lower-resolution components (Mallat 1989).

The streamflow data is decomposed into an approximation and eight detail (D) components. For station 1413, time series of 2-monthly mode (D1), 4-monthly mode (D2), 8-monthly mode (D3), 16-monthly mode (D4), 32-monthly mode (D5), 64-monthly mode (D6), 128-monthly mode (D7), and 256-monthly mode (D8) are presented in Figure 2. D1 presents the lowest-frequency component. Each of D components has different effects on the observed flow series. The correlation coefficients between each of the D components and the observed streamflows are computed and presented in Table 2 for station 1413. This provides information for the input selection of neuro-fuzzy model and for the determination of effective wavelet components on observed streamflow.

According to the correlation results (Table 2), for the correlation between $(t-1)$-time D series and t-time measured monthly streamflow series, D3 component shows the highest correlation (equal to 0.659). Also, D2, D4, D5, D6, D7 show relatively high correlation coefficients. Similarly, for the correlation between $(t-2)$-time D series and t-time measured monthly streamflow series, the D3 component shows the highest correlation value (its value is 0.356). Additionally, D4, D5, D6 and D7 components show slightly higher correlation than the others. For the correlation between the D series at time $t-3$ and measured monthly streamflow series at time t, D2 component shows the highest correlation value but it is negative. On the other hand, D6 shows the highest positive correlation value (0.260). In order to select dominant D components, average correlations are evaluated. The average correlations are given in the last column of Table 2. According to the average correlations, the D3, D4, D5, D6 and D7 components seem to be more effective than the others.

The correlation analysis on the periodic components reveals the component which is more effective on the original streamflow data. The determined D components are added to each other so that the new series is obtained. For the station 1413, the $D3+D4+D5+D6+D7$ components are used as inputs for conjunction model.

Monthly streamflow forecasting

Two different approaches are studied for monthly streamflow forecasting.

First, the neuro-fuzzy model is employed using the previous observed monthly streamflow inputs. Here, data is

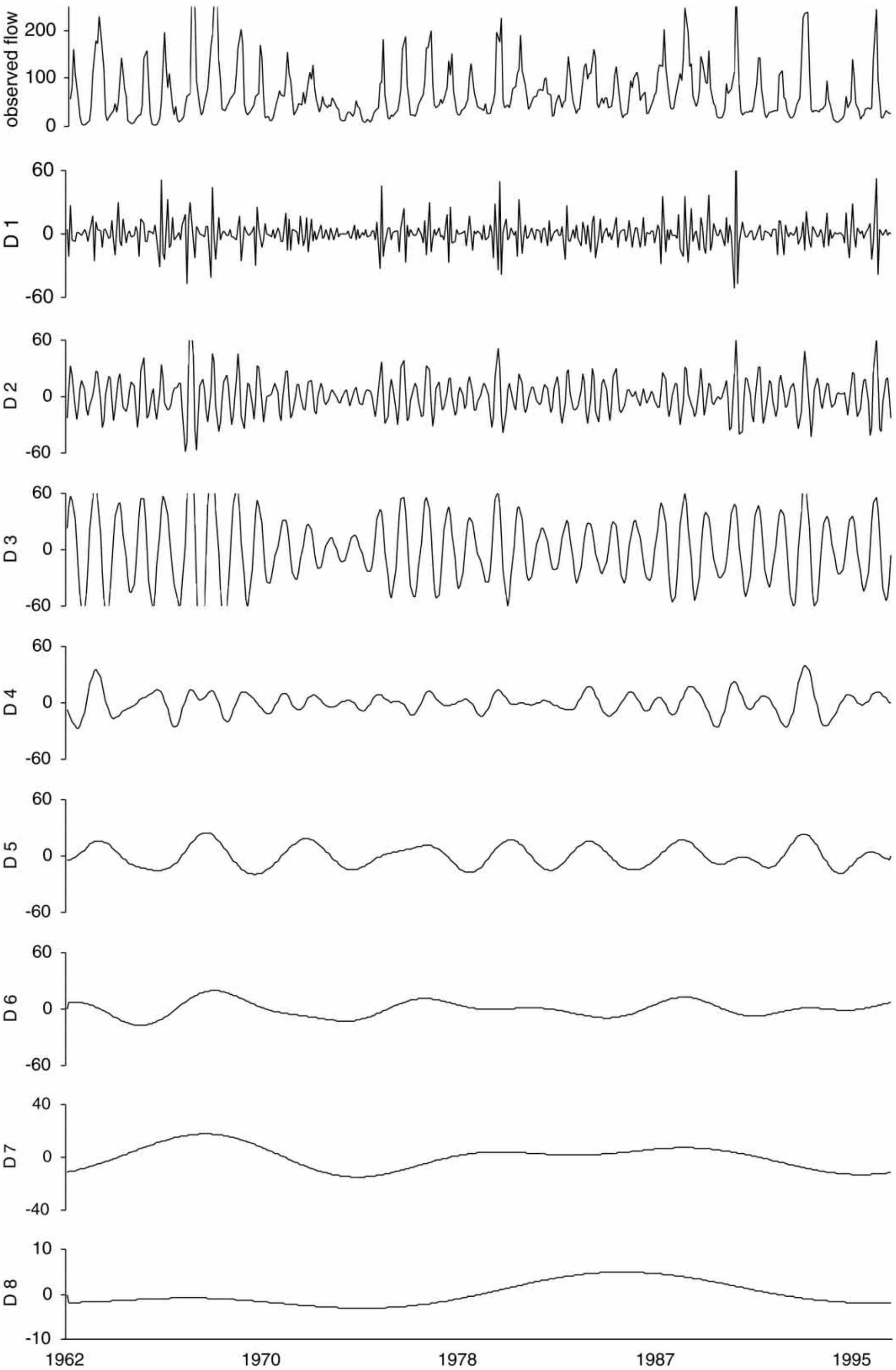

Figure 2 | Decomposed wavelet sub-time series at station 1413.

divided into two parts, training and testing periods. In the applications, the first 26 years of flow data (336 months, 80% of the whole data set) are used for training and the remaining seven years (84 months, 20% of the whole data set) are used for testing. The inputs represent the previous monthly streamflows (at time $t-1$, $t-2$ and $t-3$) and the

Table 2 | The correlation coefficients between each of sub-time series and original monthly flow data for 1413 station

Discrete wavelet components	Correlation coefficient	Correlation between *t* − 1 time D series and *t*-time measured monthly flow	Correlation between *t* − 2 time D series and *t*-time measured monthly flow	Correlation between *t* − 3 time D series and *t*-time measured monthly flow	Average correlations
D1	0.342	−0.128	−0.089	0.030	0.039
D2	0.565	0.293	−0.180	−0.350	0.082
D3	0.773	0.659	0.356	−0.038	0.438
D4	0.452	0.419	0.326	0.197	0.349
D5	0.320	0.316	0.302	0.283	0.305
D6	0.272	0.271	0.266	0.260	0.267
D7	0.225	0.224	0.225	0.230	0.226
D8	0.126	0.126	0.129	0.131	0.128
Approximate	0.050	0.050	0.050	0.052	0.050

output corresponds to the monthly streamflow at time t. Thus, the three different input combinations evaluated for streamflow forecasting are (i) Q_{t-1}; (ii) Q_{t-1} and Q_{t-2}; (iii) Q_{t-1}, Q_{t-2}, and Q_{t-3}.

The performance evaluation measures are the root mean square errors (RMSE), mean absolute relative errors (MARE) and coefficient of determination (R^2) between forecast and observed streamflows. The R^2 measures the degree to which two variables are linearly related. RMSE and MARE provide different types of information about the predictive capabilities of the model. The MSE measures the goodness-of-fit relevant to high flow values whereas the MARE yields a more balanced perspective of the goodness-of-fit at moderate flows (Karunanithi *et al.* 1994). The RMSE and MARE are defined as

$$\mathrm{RMSE} = \sqrt{\sum_{i=1}^{N} \frac{1}{N} (Yi_{\mathrm{observed}} - Yi_{\mathrm{estimate}})^2} \tag{5}$$

$$\mathrm{MARE} = \frac{1}{N} \sum_{i=1}^{N} \frac{|Yi_{\mathrm{observed}} - Yi_{\mathrm{estimate}}|}{Yi_{\mathrm{observed}}} 100 \tag{6}$$

in which N is the number of data set and Y_i is the monthly streamflow.

The RMSE, MARE and R^2 statistics of different neuro-fuzzy applications in test period are summarized in Table 3. For station 1413, Table 3 indicates that the neuro-fuzzy model whose inputs are the flows of two previous months (input combination (ii)) has the best accuracy. For station 2015, the model with three previous monthly streamflow inputs (Q_{t-1}, Q_{t-2}, and Q_{t-3}) showed the best forecast performance from the RMSE and MARE viewpoints (RMSE = 2.39 m^3/s, MARE = 21.4).

Secondly, the wavelet-neuro-fuzzy model is employed for monthly streamflow forecasting. Here, the neuro-fuzzy model is evaluated with the inputs comprising the wavelet sub-series of the observed monthly streamflows. The new series obtained by adding D3, D4, D5, D6 and D7 components are used for forecasting. Namely, the summed wavelet components (the new series) instead of original data are employed as inputs to the neuro-fuzzy model for the monthly streamflow forecasting. Here also the data are divided into two parts as training and testing periods as mentioned in the previous application. The accuracies of

Table 3 | The RMSE, MARE and R^2 statistics of different neuro-fuzzy applications in test period

Model input		1413			2015		
		RMSE, (m^3/s)	MARE, (%)	R^2	RMSE, (m^3/s)	MARE, (%)	R^2
(i)	Q_{t-1}	43.5	52.2	0.460	3.29	28.8	0.524
(ii)	Q_{t-1} and Q_{t-2}	39.8	45.7	0.550	2.46	21.8	0.751
(iii)	Q_{t-1}, Q_{t-2} and Q_{t-3}	41.5	47.3	0.538	2.39	21.4	0.745

wavelet-neuro-fuzzy models for three input combinations including the summed wavelet components in test period are given in Table 4. It can be seen from this table that the wavelet-neuro-fuzzy model whose inputs are the flows of three previous months (input combination (iii)) performs the best for both stations. Tables 3 and 4 indicate that the wavelet decomposition significantly increases the accuracy of the neuro-fuzzy model from the RMSE, MARE and R^2 viewpoints. For stations 1413 (respectively 2015) the reductions in the RMSE and MARE are 41% (respectively

Table 4 | The RMSE, MARE and R^2 statistics of different wavelet- neuro-fuzzy applications in test period (using wavelet coefficients inputs)

Model input		1413			2015		
		RMSE, (m³/s)	**MARE, (%)**	R^2	**RMSE, (m³/s)**	**MARE, (%)**	R^2
(i)	D_{t-1}	38.0	61.8	0.590	3.19	33.6	0.585
(ii)	D_{t-1} and D_{t-2}	25.1	39.5	0.826	1.56	23.2	0.931
(iii)	D_{t-1}, D_{t-2} and D_{t-3}	23.4	26.1	0.849	1.32	19.3	0.954

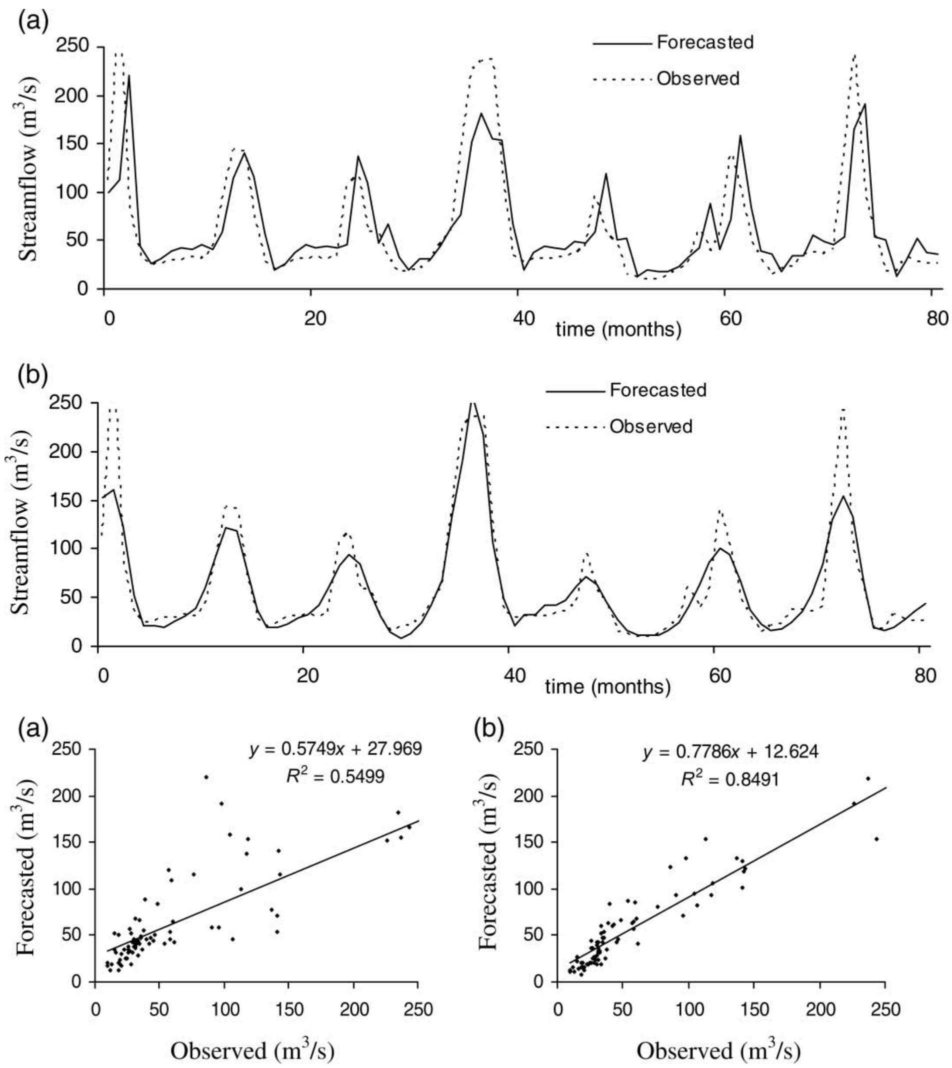

Figure 3 | Observed and forecasted streamflow using (a) neuro-fuzzy and (b) wavelet-neuro-fuzzy model at station 1413 for test period.

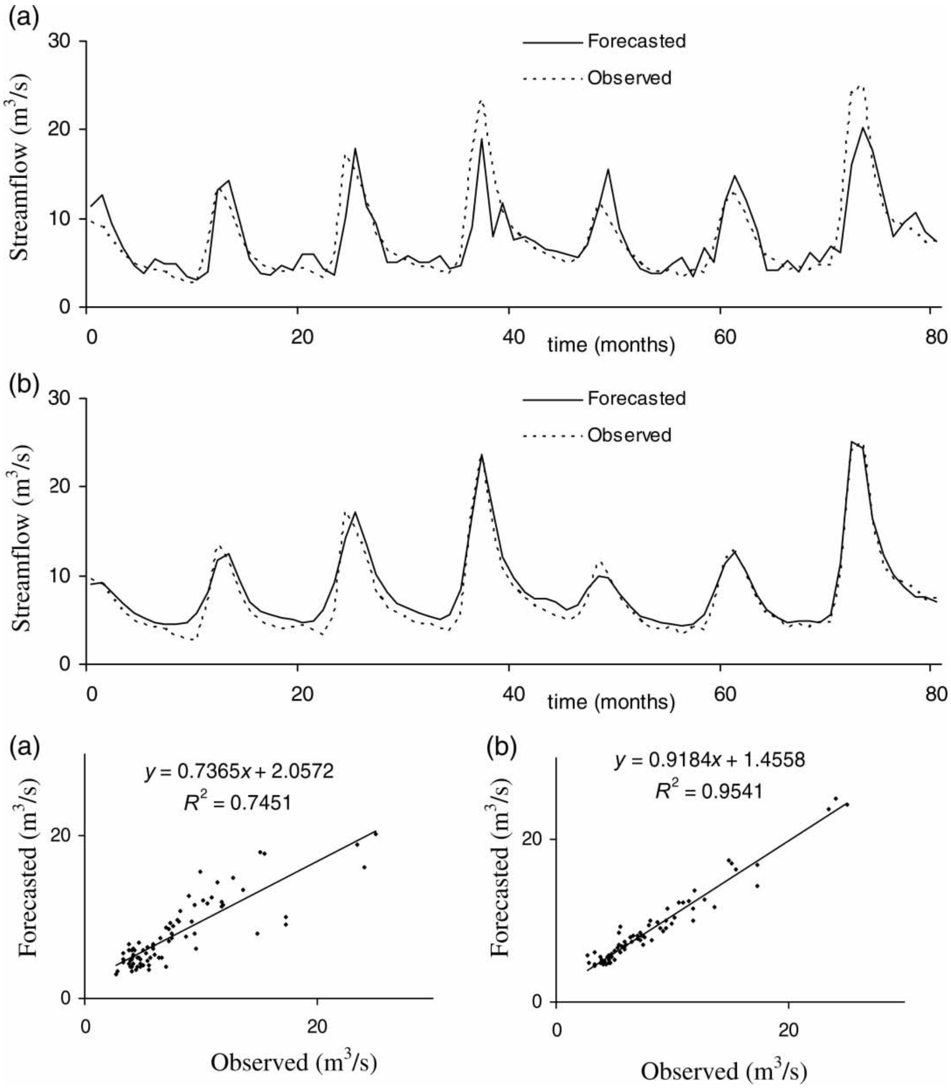

Figure 4 | Observed and forecasted streamflow using (a) neuro-fuzzy and (b) wavelet-neuro-fuzzy model at station 2015 for test period.

45%) and 43% (respectively 10%) and the increment in the R^2 is 54% (respectively 28%).

For station 1413, the model estimates in the test period are compared with the observed monthly flows in Figure 3 in the form of hydrograph and scatterplot. As seen from Figure 3, the wavelet-neuro-fuzzy model approximates the general behavior of the observed hydrographs. As can be seen from the fit line equations (assume that the equation is $y = a_0x + a_1$) in the scatterplots, the a_0 and a_1 coefficients for the wavelet-neuro-fuzzy model model are respectively closer to the 1 and 0 with a higher R^2 value of 0.849 than those of the neuro-fuzzy model. It can be obviously seen from the scatterplots that the estimates of conjunction model are less scattered. The forecasting performances of the wavelet-neuro-fuzzy and neuro-fuzzy models are compared in Figure 4 for station 2015. It can be obviously seen from the hydrographs that the conjunction model provides much closer estimates to the corresponding observed flow values than does the neuro-fuzzy model. Particularly, the peaks in the test period are forecasted satisfactorily by the wavelet-neuro-fuzzy model. The superiority of the wavelet-neuro-fuzzy model can also be seen from the scatterplots. The a_0 and a_1 coefficients of fit line equation for the wavelet-neuro-fuzzy model are respectively closer to the 1 and 0 with a higher R^2 value of 0.954 than those of the neuro-fuzzy model as found for the station 1413.

CONCLUSIONS

In this study, the ability of wavelet-neuro-fuzzy model for streamflow forecast has been investigated. Streamflow forecast with wavelet-neuro-fuzzy model has been employed for the first time.

Two different approaches were used for monthly streamflow forecast. First, the neuro-fuzzy model was employed using the previous observed monthly streamflow inputs. Secondly, the wavelet-neuro-fuzzy model was employed for the monthly streamflow forecasting. The streamflow data was decomposed into sub-series by discrete wavelet transform. One of the important difficulties for a forecast model is determining the appropriate model inputs. The correlation coefficients between wavelet components and observed streamflow series were evaluated for the selection of appropriate components. Thus, the obtained new series (D3 + D4 + D5 + D6 + D7) were selected as the conjunction model inputs. Then, the wavelet-neuro-fuzzy model was constructed with new series as inputs and the observed streamflow series as output. The results show that the performance of the conjunction method (the wavelet-neuro-fuzzy model) is superior to classical neuro-fuzzy model. The wavelet decomposition significantly increased the accuracy of the neuro-fuzzy model. Particularly, peaks (high monthly flows) in the test period were forecast satisfactorily by the wavelet-neuro-fuzzy model.

By the discrete wavelet transform, original signals are represented by different resolution interval. Some properties of the sub-series such as its daily, monthly, and annual periods can be seen more clearly than in the original signal. With appropriate sub-series belonging to different scales, the neuro-fuzzy model is constructed. Because the features (such as periodicity) of these sub-series are obvious, forecasts are more accurate than those obtained directly by original signals (Ning & Yunping 1998).

The method combining discrete wavelet transform and the neuro-fuzzy model provides a new access to forecasting problems. Wavelet analysis positively affects the forecast ability of the neuro-fuzzy approach.

REFERENCES

Alp, M. & Cigizoglu, H. K. 2007 Suspended sediment load simulation by two artificial neural network methods using hydrometeorological data. *Env. Modell. Softw.* **22**, 2–13.

Anctil, F. & Tape, D. G. 2004 An exploration of artificial neural network rainfall-runoff forecasting combined with wavelet decomposition. *J. Env. Engng Sci.* **3**, S121–S128.

Antar, M. A., Elassioitti, İ. & Allam, M. N. 2006 Rainfall-runoff modelling using artificial neural networks technique: a Blue Nile catchment case study. *Hydrol. Proccess.* **20** (5), 1201–1216.

Cannas, B., Fanni, A., See, L. & Sias, G. 2006 Data processing for river flow forecasting using neural networks: wavelet transforms and data partitioning. *Phys. Chem. Earth* **31**, 1164–1171.

Chang, F. J. & Chang, Y. T. 2006 Adaptive neuro-fuzzy inference system for prediction of water level in reservoir. *Adv. Wat. Res.* **29**, 1–10.

Cigizoglu, H. K. 2005 Application of the generalized regression neural networks to intermittent flow forecasting and estimation. *ASCE J. Hydrol. Engng* **10** (4), 336–341.

Cigizoglu, H. K. & Kisi, O. 2006 Methods to improve the neural network performance in suspended sediment estimation. *J. Hydrol.* **317** (3–4), 221–238.

Coulibaly, P. & Burn, H. D. 2004 Wavelet analysis of variability in annual Canadian streamflows. *Water Resources Res.* **40**, W03105.

Daubechies, I. 1990 The wavelet transform, time-frequency localization and signal analysis. *IEEE Trans. Inform. Theor.* **36**, 961–1005.

Drake, J. T. 2000 *Communications Phase Synchronization Using The Adaptive Network Fuzzy Inference System*. PhD Thesis, New Mexico State University, Las Cruces, NM.

Freiwan, M. & Cigizoglu, H. K. 2005 Prediction of total monthly rainfall in Jordan using feed forward backpropagation method. *Fresenius Env. Bull.* **14** (2), 142–151.

Hall, T. 1999 Precipitation forecasting using a neural network. *Weather Forecasting* **14**, 338–345.

Hsu, K., Gupta, H. V. & Sorooshian, S. 1995 Artificial neural network modelling of the rainfall runoff process. *Water Resources Res.* **31**, 2517–2530.

Iliadis, L. S. & Maris, F. 2007 An Artificial Neural Network model for mountainous water-resources management: the case of Cyprus mountainous watersheds. *Env. Modell. Softw.* **22**, 1066–1072.

Jang, J. S. R. 1993 ANFIS: adaptive-network-based fuzzy inference system. *IEEE Trans. Syst. Manage. Cybernet.* **23** (3), 665–685.

Jang, J. S. R., Sun, C.-T. & Mizutani, E. 1997 *Neuro-Fuzzy and Soft Computing: A Computational Approach to Learning and Machine Intelligence*. Prentice-Hall, Upper Saddle River, NJ.

Karunanithi, N., Grenney, W. J., Whitley, D. & Bovee, K. 1994 Neural networks for river flow prediction. *J. Comp. Civil Engng ASCE* **8** (2), 201–220.
Kim, T. W. & Valdes, J. B. 2003 Nonlinear model for drought forecasting based on a conjunction of wavelet transforms and neural networks. *ASCE J. Hydrol. Engng* **6**, 319–328.
Kisi, O. 2004a River flow modeling using artificial neural networks. *ASCE J. Hydrol. Engng* **9**, 60–63.
Kisi, O. 2004b Multi-layer perceptrons with Levenberg–Marquardt training algorithm for suspended sediment concentration prediction and estimation. *Hydrol. Sci. J.* **49** (6), 1025–1040.
Kisi, O. 2005 Suspended sediment estimation using neuro-fuzzy and neural network approaches. *Hydrol. Sci. J.* **50** (4), 683–696.
Kisi, O. 2006 Daily pan evaporation modelling using a neuro-fuzzy computing technique. *J. Hydrol.* **329**, 636–646.
Kisi, O. 2008 River flow forecasting and estimation using different artificial neural network techniques. *Hydrol. Res.* **39** (1), 27–40.
Kisi, O. & Ozturk, O. 2007 Adaptive neuro-fuzzy computing technique for evapotranspiration estimation. *ASCE J. Irrig. Drain. Engng* **133** (4), 368–379.
Kumar, D. N., Raju, K. S. & Sathish, T. 2004 River flow forecasting using recurrent neural network. *Water Resources Manage.* **18**, 143–161.
Kucuk, M. 2004 *Modelling River Flow Series Using Wavelet Transform*. PhD Thesis, Istanbul Technical University (in Turkish).
Küçük, M. & Ağıralioğlu, N. 2003 Stationary and non-stationary time series analysis aided by short time Fourier transform. III. *National Atmosphere Symposium*, March, 19–21 March, Istanbul, Turkey.
Li, X., Ding, J. & Li, H. 1999 Combining neural network models based on wavelet transform. *J. Hydraul.* **2**, 1–4 (in Chinese).
Lu, R. Y. 2002 Decomposition of interdecadal and interannual components for North China rainfall in rainy season. *Chin. J. Atmos.* **26**, 611–624 (in Chinese).
Mallat, S. G. 1989 A theory for multi resolution signal decomposition: The wavelet representation. *IEEE Trans. Pattern Analysis and Machine Intelligence* **11** (7), 674–693.
Mallat, S. A. 1998 *Wavelet Tour of Signal Processing*. Academic Press, San Diego.
May, D. B. & Sivakumar, M. 2009 Prediction of urban stormwater quality using artificial neural networks. *Env. Model. Softw.* **24**, 296–302.
Nayak, P. C., Sudheer, K. P., Rangan, D. M. & Ramasastri, K. S. 2004 A neuro-fuzzy computing technique for modeling hydrological time series. *J. Hydrol.* **291** (1–2), 52–66.
Nayak, P. C., Sudheer, K. P., Rangan, D. M. & Ramasastri, K. S. 2005 Short-term flood forecasting with a neurofuzzy model. *Wat. Res. Res.* **41** (4), W04004.
Ning, M. & Yunping, C. 1998 An ANN and wavelet transformation based method for short term load forecast. Energy management and power delivery. In: *International Conferences*, vol. 2, pp. 405–410.
Park, J. & Mann, M. E. 2000 Interannual temperature events and shifts in global temperature: a multiple wavelet correlation approach. *Earth Interact.* **19**, 391–403.
Partal, T. & Kisi, O. 2007 Wavelet and neuro-fuzzy conjunction model for precipitation forecasting. *J. Hydrol.* **347**, 199–212.
Partal, T. & Küçük, M. 2006 Long-term trend analysis using discrete wavelet components of annual precipitations measurements in Marmara region (Turkey). *Phys. Chem. Earth* **31**, 1189–1200.
Ramirez, M. C. V., Velho, H. F. C. & Ferreira, N. J. 2005 Artificial neural network technique for rainfall forecasting applied to the Sao Paulo region. *J. Hydrol.* **301**, 146–162.
Sivakumar, B. 2005 Hydrologic modeling and forecasting: role of thresholds. *Env. Modell. Softw.* **20**, 515–519.
Sivakumar, B., Jayawerdana, A. W. & Fernando, T. M. K. G. 2002 River flow forecasting: use of phase-space reconstruction and artificial neural networks approaches. *J. Hydrol.* **265**, 225–245.
Smith, L. C., Turcotte, D. L. & Isacks, B. 1998 Stream flow characterization and feature detection using a discrete wavelet transform. *Hydrol. Process.* **12**, 233–249.
Tokar, A. S. & Johnson, P. A. 1999 Rainfall-runoff modelling using artificial neural networks. *J. Hydrol. Engng* **4**, 232–239.
Torrence, C. & Compo, G. P. 1998 A practical guide to wavelet analysis. *Bull. Am. Meteorol. Soc.* **79**, 61–78.
Xingang, D., Ping, W. & Jifan, C. 2003 Multiscale characteristics of the rainy season rainfall and interdecadal decaying of summer monsoon in North China. *Chin. Sci. Bull.* **48**, 2730–2734.
Wang, D. & Ding, J. 2003 Wavelet network model and its application to the prediction of hydrology. *Nat. Sci.* **1**, 67–71.
Yan, Z., Tsimplis, M. N. & Woolf, D. 2004 Analysis of the relationship between the North Atlantic oscillation and sea level changes in northeast Europe. *Int. J. Climatol.* **24**, 743–758.
Yueqing, X., Shuangcheng, L. & Yunlong, C. 2004 Wavelet analysis of rainfall variation in the Hebei Plain. *Sci. Chin. D Earth Sci.* **48**, 2241–2250.
Zealand, C. M., Burn, D. H. & Simonovic, S. P. 1999 Short term streamflow forecasting using artificial neural networks. *J. Hydrol.* **214**, 32–48.
Zhang, B. L. & Dong, Z. Y. 2001 An adaptive neural-wavelet model for short term load forecasting. *Electric Power Syst. Res.* **59**, 121–129.
Zheng, T., Girgis, A. A. & Makram, E. B. 2000 A hybrid wavelet Kalman filter method for load forecasting. *Electric Power Syst. Res.* **54**, 11–17.

First received 24 May 2010; accepted in revised form 15 September 2010. Available online July 2011